

S2TX: Cross-Attention Multi-Scale State-Space Transformer for Time Series Forecasting

Zihao Wu¹ Juncheng Dong^{1*} Haoming Yang^{1*} Vahid Tarokh¹

Abstract

Time series forecasting has recently achieved significant progress with multi-scale models to address the heterogeneity between long and short range patterns. Despite their state-of-the-art performance, we identify two potential areas for improvement. First, the variates of the multivariate time series are processed independently. Moreover, the multi-scale (long and short range) representations are learned separately by two independent models without communication. In light of these concerns, we propose *State Space Transformer with cross-attention* (S2TX). S2TX employs a cross-attention mechanism to integrate a Mamba model for extracting long-range cross-variate context and a Transformer model with local window attention to capture short-range representations. By cross-attending to the global context, the Transformer model further facilitates variate-level interactions as well as local/global communications. Comprehensive experiments on seven classic long-short range time-series forecasting benchmark datasets demonstrate that S2TX can achieve highly robust SOTA results while maintaining a low memory footprint.

1. Introduction

Forecasting multivariate time series represents a core learning paradigm designed to predict upcoming time steps using historical data. This machine learning task finds application across a range of domains including the economy (Koop et al., 2010), epidemiology (Nguyen et al., 2021), and meteorology (Angryk et al., 2020). Due to its significant influence, multivariate time series forecasting has garnered considerable focus. State-of-the-art (SOTA) methods for multivariate time series forecasting predominantly utilize two types of sequence models: transformers and state-space

*Equal contribution ¹Department of Electrical and Computer Engineering, Duke University, Durham, NC 27708, USA. Correspondence to: Zihao Wu <zihao.wu@duke.edu>.

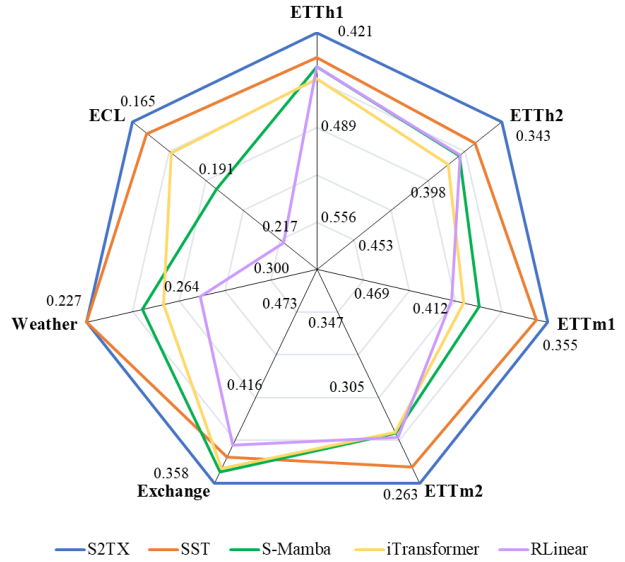


Figure 1. Overview of the performance of different architectures over 7 different benchmark datasets. Average results (MSE) are reported.

models (Vaswani, 2017; Gu & Dao, 2023). By employing these foundational structures, researchers aim to advance this research domain by harnessing two key features of multivariate time series: 1) identifying temporal dependencies and 2) understanding inter-variate correlations. Effectively integrating both temporal dynamics and the interactions between variates within a single learning model is essential for the precise forecasting of these intricate multivariate time series (Box et al., 2015).

A recent advancement Xu et al. (2024) integrates transformers and state-space models within a multi-scale framework: it first breaks down the input time series into shorter high resolution *patches* and longer low resolution patches. Subsequently, it feeds the high resolution patches into a transformer model with local-attention to extract fine-grained local features and the low resolution longer patches to a state-space model (i.e., Mamba (Gu & Dao, 2023)) to learn long-range global features. This multi-scale mixture of Mamba and transformer models greatly improves the mod-

eling of temporal dependencies. However, it leaves a crucial aspect of multivariate time series forecasting unattended, that is, the correlation between variates. Additionally, the local and global features are modeled independently, which overlooks the interplay between global and local features. Such global-local interplay is manifested in many real-world scenarios. For example, the commonly known *El Niño* effect is a global, long-term weathering effect in the time-scale of years; but this global weather pattern will greatly affect the short-term local time series within days (Hsieh, 2004).

The cross-variate correlation and global-local features interplay, illustrated in Figure 2, are two crucial aspects of multivariate time series forecasting. Global patterns encompassed in the purple boxes consistently suggest increased local variation while the red-boxed region indicates a strongly inversed correlation between the two variates. To explicitly include these two crucial aspects, we introduce *State Space Transformer with Cross-attention* (S2TX) where we connect cross-variate global features with fine grained local features through a carefully designed cross-attention mechanism. Specifically, we apply Mamba as the global model to process long-range, low-resolution patches across all variates in a single sweep, extracting cross-variate global context. This global context is then provided as the key and value for cross-attention to a decoder-like transformer model focusing on local, high-resolution, variate-independent patches.

Contributions. Our contributions are summarized below:

- We identify two crucial aspects, cross-variate correlation and global-local interaction, to improve the SOTA time series forecasting model.
- We propose a novel multi-scale architecture that incorporates these considerations through a cross-attention mechanism. In particular, our architecture learns variate-level correlation while leveraging the enhanced temporal learning of patchification.
- We develop a cross-attention mixture of experts, enabling global-local feature interplay between a global feature-focused state-space model and a local feature-focused transformer model.
- We verify the efficacy of our proposed architecture on a comprehensive set of time series forecasting benchmarks.

2. Related Works

The field of time series forecasting has seen significant evolution over the decades: shifting from classical mathematical tools (Bloomfield, 2004; Durbin & Koopman, 2012) and statistical techniques like ARIMA (Nerlove, 1971; Hyndman, 2018) to more recent deep learning approaches such

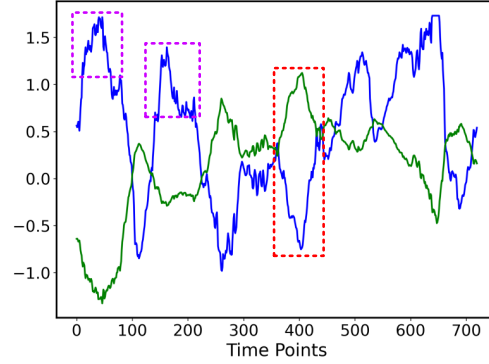


Figure 2. A snippet of the weather dataset. Two variables (blue and green) were plotted over 720 time steps. The purple boxed region indicates where a global-local interaction exists, and the red boxed region indicates a cross-variate correlation.

as recurrent neural networks (Graves et al., 2013) and long-short term memory models (Gers et al., 2000). Notably, in recent years, transformers (Vaswani, 2017) have demonstrated particularly promising performance on sequence modeling tasks, especially in natural language processing. Interestingly, studies have revealed that even simple linear layers can outperform complex transformer-based models in both performance and efficiency for time series forecasting (Zeng et al., 2023; Yang et al., 2024).

Inverted Dimension. In investigating why transformers underperform in time series forecasting, Liu et al. (2023) argues that the direct application of transformers that embed all variates is undesirable. This embedding compresses variates with distinct physical meanings and inconsistent measurement at each time step to a single token, erasing the important multivariate correlations. To address this limitation, the authors propose inverting the dimension of time and variates in the data while preserving the core mechanisms of the transformer. Many subsequent studies (Wang et al., 2025; Ahamed & Cheng, 2024; Xu et al., 2024) build upon this paradigm, achieving improvements in both performance and efficiency.

Patchification. Patchification of inverted data transforms the time series of each variate into a multivariate time sequence where the patches are stacked to construct an additional dimension. While patchification facilitates the capture of temporal dependencies by introducing an inductive bias aligned with the localized nature of time series data, it also overlooks the between-variate correlations due to the additional dimension: existing approaches, such as SST (Xu et al., 2024) and PatchTST (Nie et al., 2022), treat each variate independently. Despite their strong performance, these methods lack any form of inter-variate communication.

Mixture of Experts. The mixture of experts method re-

ceives increasing attention in sequence modeling after the release of Mamba (Gu & Dao, 2023). Combining the linear complexity of Mamba and the strong performance of transformers could lead to efficient and accurate sequence models. For instance, Jamba (Lieber et al., 2024) employs a layerwise stacking of Mamba and attention layers, achieving superior performance in natural language processing compared to either component individually. For time series forecasting, SST (Xu et al., 2024) utilizes Mamba to capture global patterns with prolonged patch lengths, while leveraging transformer to learn local details with shorter patch lengths. However, global and local patches are processed separately through each expert before their output embeddings are concatenated. Such inadequate communication between global and local features limits the integration results, restricting the model’s ability to fully exploit each expert’s complementary strength.

3. Preliminary

In this section, we first formalize the modeling problem, then introduce the two main modules of our proposed architecture: state-space models and cross-attention.

3.1. Problem Setup

We consider the standard problem setup for time series forecasting framework (Liu et al., 2023). Given a D -dimensional multivariate time series of length L (look-back window) $\mathbf{X} \in \mathbb{R}^{D \times L}$, the goal is to predict $\mathbf{Y} \in \mathbb{R}^{D \times H}$, the same D -dimensional multivariate time series in the future H steps (horizon length). Assuming we have access to a training dataset with N observations $\{\mathbf{X}^{(i)}, \mathbf{Y}^{(i)}\}_{i=1}^N$, our goal is to learn a function $f_\phi(\mathbf{X}^{(i)}) : \mathbb{R}^{D \times L} \rightarrow \mathbb{R}^{D \times H}$ with parameter ϕ such that the mean squared error loss is minimized:

$$\mathcal{L}_{\text{train}} = \frac{1}{N} \sum_{n=1}^N \|f_\phi(\mathbf{X}^{(i)}) - \mathbf{Y}^{(i)}\|_F^2, \quad (1)$$

where F denotes the Frobenius norm (Horn & Johnson, 2012).

3.2. State-Space Models

State-Space Models (SSMs) (Gu et al., 2020; 2021) are a family of sequence models inspired by continuous control systems described by the following equations

$$dh = Ah + Bx, z = Ch + Dx, \quad (2)$$

where $x \in \mathbb{R}$ represents a one-dimensional input, $h \in \mathbb{R}^{d \times 1}$ is the hidden state, z is the model output, $A \in \mathbb{R}^{d \times d}$, $B \in \mathbb{R}^{d \times 1}$, $C \in \mathbb{R}^{1 \times d}$, and $D \in \mathbb{R}^{1 \times 1}$ are parameter matrices. Matrix D acts as a skip connection and is typically omitted in derivations. For multi-dimensional inputs, a

stack of SSMs is employed. The continuous system is then discretized into

$$h_{t+1} = \bar{A}h_t + \bar{B}x_t, z_{t+1} = \bar{C}h_t, \quad (3)$$

where the discretized matrices are obtained with a discretization rule and a step size Δ . For example, Mamba (Gu & Dao, 2023) uses Zero-Order Holder rule such that $\bar{A} = \exp(\Delta A)$, $\bar{B} = \exp(\Delta A)^{-1}(\exp(\Delta A) - \mathbb{I}) \cdot \Delta B$.

The discretized state-space models can be interpreted either as a convolutional neural network, enabling linear-time parallel training, or as a linear recurrent neural network, supporting constant-time inference, as demonstrated in S4 (Gu et al., 2021). Building upon S4, Mamba extends this approach by making the matrices B and C input-dependent, transforming them into a selective SSM. Additionally, Mamba introduces a parallel scan algorithm to achieve linear-time training complexity.

3.3. Cross-attention

Cross-attention is a generalization (Bahdanau, 2014) of self-attention (Vaswani, 2017). Given source data $S \in \mathbb{R}^{L_S \times d_{\text{model}}}$ and target data $T \in \mathbb{R}^{L_T \times d_{\text{model}}}$, the output of cross-attention is

$$\text{CrossAttention}(S, T) = \frac{(TW_q)(SW_k)^T}{\sqrt{d_{\text{model}}}} SW_v \quad (4)$$

where $W_k, W_q, W_v \in \mathbb{R}^{d_{\text{model}} \times d_{\text{model}}}$ are learnable parameters. From this perspective, self-attention can be achieved by substituting all instances of S with T in Cross-attention:

$$\text{SelfAttention}(T) = \text{CrossAttention}(T, T) \quad (5)$$

This cross-attention mechanism will allow us to compute cross-attentional weight where the influence of global patterns is weighted to predict a specific local pattern, allowing global-local interaction during inference. Notably, our application of cross-attention mechanism to integrate multi-scale features are commonly applied in computer vision tasks (Chen et al., 2021).

4. State-Space Transformer with Cross-attention

Here we describe our proposed method State-Space Transformer with Cross-attention (S2TX). We first introduce the Multi-Scale patching process that decompose a long time series into global and local patches of different time scales. The low-resolution global patches were then fed to a Mamba-based global feature extractor to obtain the cross-variate global context. The global context is then applied as the key and value for a novel global-local cross-attention to improve the extraction of local features. Finally, we conduct

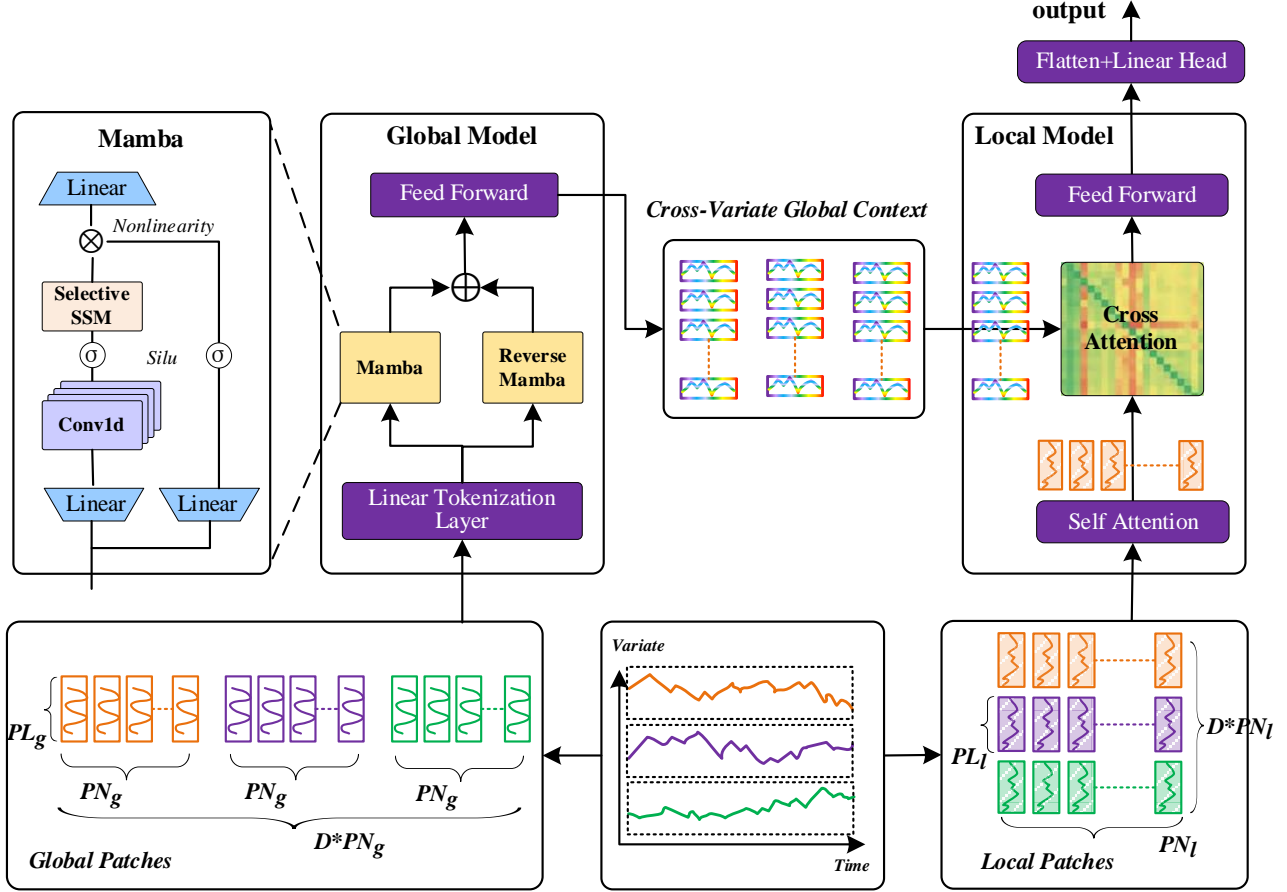


Figure 3. Overview of the proposed architecture S2TX. Different variables (in different colors) of the time series are patched into global and local patches. The global patches are processed by the global model, which outputs the global context that is used to compute the key and value matrices during cross-attention with the local model. Skip connections and normalization layers are omitted for clarity of presentation.

a computation complexity analysis, showcasing that S2TX, with the addition of our novel cross-attention, maintained a low-memory footprint during training and inference. The general structure of S2TX is provided in Figure 3.

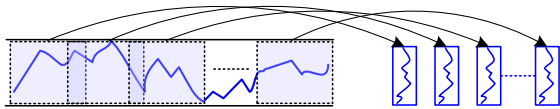


Figure 4. Patch transforms a one-dimensional sequence to a sequence of patches.

4.1. Multi-Scale Patch

The patching technique has become increasingly popular for time series forecasting (Gong et al., 2023; Nie et al., 2022; Xu et al., 2024). It aggregates local information into

patches and effectively enhances the receptive field. Denote the sequence length of the look-back window by L , patch length by PL , stride by STR , and patch number by PN , where

$$PN = \left\lceil \frac{L - PL}{STR} \right\rceil. \quad (6)$$

The patching technique transforms each (one-dimensional) variate of length L into a PL -dimensional time series of length PN . More specifically, the input time series $\mathbf{X} \in \mathbb{R}^{D \times L}$ is patched into $\tilde{\mathbf{X}} \in \mathbb{R}^{D \times PN \times PL}$.

Intuitively the longer the stride, or the longer the patch length, the more long range temporal context is stored in a patch and vice versa. Utilizing this intuition, we apply the patching process onto the time series *twice*: (i) one of them focuses on coarser granularity for global context, employing the full look-back window of length L , a larger patch length PL_g and longer stride, along with the corre-

sponding patch number PN_g to obtain long-range global time series patches; (ii) the other leverages finer granularity with a fixed shorter look-back window of length S , a smaller patch length PL_l , and shorter stride with corresponding patch number PN_l to obtain short-range local patches. The resulting two multi-scale time series patches $\tilde{\mathbf{X}}_g \in \mathbb{R}^{D \times PN_g \times PL_g}$ and $\tilde{\mathbf{X}}_l \in \mathbb{R}^{D \times PN_l \times PL_l}$ serve as inputs for the global and local models, respectively.

4.2. Cross-Variate Global Context

The global patches $\tilde{\mathbf{X}}_g$ is first passed through the global feature extractor, which is a dual Mamba system, responsible for cross-variate global feature extraction. We begin by concatenating along the first and second dimension of $\tilde{\mathbf{X}}_g$, viewed with a new shape $\tilde{\mathbf{X}}_g \in \mathbb{R}^{(D * PN_g) \times PL_g}$ as illustrated in Figure 4. This allows the learning of variate-level correlation across all D dimensions as the selection mechanism of Mamba will filter the relevant variates and patches, enabling the global model to capture cross-variate global context. However, Mamba processes data unilaterally, attending only to antecedent patches, which limits learning of the full global context. Inspired by S-Mamba (Wang et al., 2025), we employ two Mamba models to scan the sequence in both forward and backward directions before aggregating the results. This approach improves the learning of correlations between global patches across variables. Specifically, we have

$$\vec{\mathbf{Z}}_g = \overrightarrow{\text{Mamba Layers}}(\tilde{\mathbf{X}}_g), \quad (7)$$

$$\overleftarrow{\mathbf{Z}}_g = \overleftarrow{\text{Mamba Layers}}(\tilde{\mathbf{X}}_g), \quad (8)$$

$$\mathbf{Z}_g = \vec{\mathbf{Z}}_g + \overleftarrow{\mathbf{Z}}_g, \quad (9)$$

where $\overleftarrow{\mathbf{X}}_g \in \mathbb{R}^{(D * PN_g) \times PL_g}$ is obtained by reversing the the first dimension of $\tilde{\mathbf{X}}_g$. The output of the global model $\mathbf{Z}_g \in \mathbb{R}^{(D * PN_g) \times d_{\text{model}}}$, which serves as an intermediary output of the entire architecture, is then fed to the local model. This intermediary output encapsulates both cross-variate and global context information.

Note that d_{model} represents the model dimension of Mamba, which aligns with the model dimension of the local model discussed in the next section.

4.3. Cross-Attention Local Context

With global and cross-variate patterns as context information, the local model can more effectively capture local features and interpret local variations. To this end, we employ a decoder-like transformer with each layer composed of a self-attention without causal masking followed by a cross-attention. Since cross-variate correlation is already captured by the context features, we now take each variate (in the first dimension) of $\tilde{\mathbf{X}}_l \in \mathbb{R}^{D \times PN_l \times PL_l}$ individually as the input

of the self-attention to relieve the computation burden of transformer. Denote the d -th variate of $\tilde{\mathbf{X}}_l$ after linear projection to d_{model} -dimension by $\tilde{\mathbf{X}}_l^d \in \mathbb{R}^{PN_l \times d_{\text{model}}}$. Similarly, the context feature $\mathbf{Z}_g \in \mathbb{R}^{(D * PN_g) \times d_{\text{model}}}$ is viewed back to $\mathbf{Z}_g \in \mathbb{R}^{D \times PN_g \times d_{\text{model}}}$ and the d -th variate $\mathbf{Z}_g^d \in \mathbb{R}^{PN_g \times d_{\text{model}}}$ is sent to the cross-attention as key and value to match the dimension of $\tilde{\mathbf{X}}_l^d$. Specifically, the cross-attention mechanism operates as follows:

$$\begin{aligned} & \text{AttentionBlock}(\tilde{\mathbf{X}}_l^d, \mathbf{Z}_g^d) \\ &= \text{CrossAttention}(\mathbf{Z}_g^d, \text{SelfAttention}(\tilde{\mathbf{X}}_l^d)), \end{aligned} \quad (10)$$

Note that we have omitted the skip connection and normalization steps for a concise presentation. The rest of the local model is the same as a regular transformer decoder as shown in the figure.

Denote the output of the local model of the d th variable to be $\mathbf{Y}_{\text{out}}^d \in \mathbb{R}^{PN_l \times d_{\text{model}}}$. Stacking the outputs of all variables, we obtain $\mathbf{Y}_{\text{out}} \in \mathbb{R}^{D \times PN_l \times d_{\text{model}}}$. The last two dimensions of \mathbf{Y}_{out} are then flattened and a final linear head is employed to project from dimension $PN_l \times d_{\text{model}}$ to H , which is the target horizon window.

4.4. Runtime Complexity Analysis

The Mamba layers, which exhibit linear complexity, process a sequence of length $D \cdot PN_g$ with a complexity of $O(D \cdot PN_g)$, which is linear to input time series length L due to definition of PN in Equation (6). On the other hand, while transformer models exhibit quadratic complexity with respect to sequence length, S2TX uses a local look-back window with fixed length S , resulting in a complexity of $O(D \cdot PN_l^2) = O(D)$ as $PN_l = O(S) = O(1)$. Thus, S2TX has an overall linear complexity with respect to L and D . Moreover, as L increases, we can proportionally increase both the patch length and stride so that PN_g remains constant, in which case, the overall complexity of S2TX reduces to constant order with respect to L while remaining linear order with respect to D . Our empirical results in Section 5.3 verifies this, showing that S2TX’s runtime barely increases with L .

5. Experiment

We empirically demonstrate that utilizing cross-variate correlation and global-local interaction can significantly improve the forecasting performance. We first introduce the experimental setup, then we showcase the performance of S2TX over a variety of benchmark against recent state-of-the-art architectures. We then demonstrate the efficacy of the main component of S2TX with a set of ablation study and a robustness study where we test the robustness of S2TX with sequences of missing values. Finally, we showcase the low memory footprint and efficient runtime of S2TX compared

S2TX: cross-attention Multi-Scale State-Space Transformer for Time Series Forecasting

	S2TX 2025		SST 2025		S-Mamba 2025		TimeM 2024		iTrans 2024		RLinear 2024		PatchTST 2023		CrossF 2023		TimesNet 2023	
	MSE	MAE	MSE	MAE	MSE	MAE	MSE	MAE	MSE	MAE	MSE	MAE	MSE	MAE	MSE	MAE	MSE	MAE
ETTh1																		
96	0.376	0.401	0.381	0.405	0.392	0.390	0.389	0.402	0.386	0.405	0.386	0.395	0.414	0.419	0.423	0.448	0.384	0.402
192	0.414	0.421	0.430	0.434	0.449	0.439	0.435	0.440	0.441	0.436	0.437	<u>0.424</u>	0.460	0.445	0.450	0.471	0.474	0.429
336	0.432	0.435	<u>0.443</u>	<u>0.446</u>	0.467	0.481	0.450	0.448	0.487	0.458	0.479	0.446	0.501	0.466	0.570	0.546	0.491	0.469
720	0.463	<u>0.473</u>	0.502	0.501	<u>0.475</u>	0.468	0.480	0.465	0.503	0.491	0.481	0.470	0.500	0.488	0.653	0.621	0.521	0.500
ETTh2																		
96	0.279	0.340	0.291	0.346	0.292	0.357	0.296	0.349	0.297	0.349	<u>0.288</u>	0.338	0.302	0.348	0.745	0.584	0.340	0.374
192	0.362	<u>0.395</u>	0.369	0.397	0.380	0.402	0.371	0.400	0.380	0.400	0.374	0.390	0.388	0.400	0.877	0.656	0.402	0.414
336	0.337	0.385	<u>0.374</u>	<u>0.414</u>	0.391	0.420	0.402	0.449	0.428	0.432	0.415	0.426	0.426	0.433	1.043	0.731	0.452	0.452
720	0.395	0.430	<u>0.419</u>	0.447	0.437	0.455	0.425	<u>0.438</u>	0.427	0.445	0.420	0.440	0.431	0.446	1.104	0.763	0.462	0.468
ETTM1																		
96	0.289	0.343	0.298	0.355	0.311	0.380	0.312	0.371	0.334	0.368	0.355	0.376	0.329	0.367	0.404	0.426	0.338	0.375
192	0.338	0.371	<u>0.347</u>	<u>0.381</u>	0.389	0.419	0.365	0.409	0.377	0.391	0.391	0.392	0.367	0.385	0.450	0.451	0.374	0.387
336	0.370	0.390	<u>0.374</u>	<u>0.397</u>	0.401	0.417	0.421	0.410	0.426	0.420	0.424	0.415	0.399	0.410	0.532	0.515	0.410	0.411
720	0.423	0.418	<u>0.429</u>	<u>0.428</u>	0.488	0.476	0.496	0.437	0.491	0.459	0.487	0.450	0.454	0.439	0.666	0.589	0.478	0.450
ETTM2																		
96	0.168	0.260	0.176	0.264	0.191	0.301	0.185	0.290	0.180	0.264	0.182	0.265	<u>0.175</u>	0.259	0.287	0.366	0.187	0.267
192	<u>0.235</u>	0.298	0.231	0.303	0.253	0.312	0.292	0.309	0.250	0.309	0.246	0.304	0.241	<u>0.302</u>	0.414	0.492	0.249	0.309
336	0.274	0.327	0.290	0.339	0.298	0.342	0.321	0.367	0.311	0.348	0.307	0.342	0.305	<u>0.343</u>	0.597	0.542	0.321	0.351
720	0.376	0.393	<u>0.388</u>	<u>0.398</u>	0.409	0.407	0.401	0.400	0.412	0.407	0.407	0.398	0.402	0.400	1.730	1.042	0.408	0.403
Exchange																		
96	0.085	<u>0.205</u>	0.097	0.222	<u>0.086</u>	0.206	0.089	0.208	0.091	0.211	0.088	0.209	0.087	0.202	0.095	0.218	0.093	0.211
192	0.179	0.303	0.191	0.315	0.182	0.304	0.184	0.309	0.182	0.303	0.188	0.311	<u>0.180</u>	0.305	0.193	0.318	0.194	0.315
336	0.311	0.402	0.337	0.424	0.330	0.416	0.333	0.416	0.337	0.421	0.346	0.423	<u>0.318</u>	<u>0.407</u>	0.359	0.429	0.358	0.433
720	0.858	0.696	0.877	0.706	0.865	0.702	0.870	<u>0.701</u>	<u>0.862</u>	0.703	0.913	0.717	0.863	0.703	0.918	0.721	0.880	0.719
Weather																		
96	0.150	0.199	<u>0.153</u>	<u>0.205</u>	0.169	0.221	0.174	0.218	0.174	0.214	0.192	0.232	0.177	0.218	0.158	0.230	0.172	0.220
192	0.194	0.242	<u>0.196</u>	<u>0.244</u>	0.205	0.248	0.200	0.258	0.221	0.254	0.240	0.271	0.225	0.259	0.206	0.277	0.219	0.261
336	<u>0.252</u>	<u>0.288</u>	0.246	0.283	0.288	0.299	0.280	0.299	0.278	0.296	0.292	0.307	0.278	0.297	0.272	0.335	0.280	0.306
720	0.313	0.333	<u>0.314</u>	<u>0.334</u>	0.335	0.369	0.352	0.359	0.358	0.347	0.364	0.353	0.354	0.348	0.398	0.418	0.365	0.359
ECL																		
96	0.134	0.231	0.141	0.239	0.157	0.255	0.156	0.240	0.148	0.240	0.201	0.281	0.181	0.270	0.219	0.314	0.168	0.272
192	0.153	0.248	<u>0.159</u>	<u>0.255</u>	0.188	0.271	0.161	0.268	0.162	0.253	0.201	0.283	0.188	0.274	0.231	0.322	0.184	0.289
336	0.170	0.266	<u>0.171</u>	<u>0.268</u>	0.192	0.275	0.195	0.272	0.178	0.269	0.215	0.298	0.204	0.293	0.246	0.337	0.198	0.300
720	0.201	0.293	<u>0.208</u>	<u>0.300</u>	0.241	0.339	0.231	0.307	0.225	0.317	0.257	0.331	0.246	0.324	0.280	0.363	0.220	0.320

Table 1. Comprehensive comparison across various datasets, prediction horizons, and baselines. The **bolded** results denote the best performance, and the underlined results indicate the second best.

to Transformer and Mamba in general.

Dataset. We benchmark our proposed algorithm S2TX on a set of 7 real-world multivariate time series datasets, including the four Electricity Transformer Temperature datasets ETTh1, ETTh2, ETTm1, and ETTm2, Weather, Electricity, and Exchange rate datasets. Detailed dataset descriptions are provided in the Appendix B.

Baselines. We benchmark our proposed algorithm S2TX against most competitive time series forecasting models within three years, including MOE-based model SST (Xu et al., 2024), Mamba-based models S-Mamba (Wang et al., 2025) and TimeMachine (TimeM) (Ahamed & Cheng, 2024), transformer-based models iTransformer (iTrans) (Liu et al., 2023), PatchTST (Nie et al., 2022), Crossformer (CrossF) (Zhang & Yan, 2023), and FEDformer (Zhou et al., 2022), linear-based models RLinear (Li et al., 2023) and DLinear (Zeng et al., 2023), and TCN-based model TimesNet (Wu et al., 2022). Due to space constraints, the comparisons against DLinear and FEDformer (pre-2023 models)

are presented in Appendix C

Experimental Setting and Metrics. For a fair comparison, the experimental setting of all baselines follows the experiment setup of the current SOTA SST. In addition, we use the same hyperparameters as in SST, including global and local patch length, stride, and look-back window. Specifically, we set $PL_g = 48$, $STR_g = 16$, $PL_l = 16$, $STR_l = 8$, and $L = 2S = 336$. For Exchange rate dataset, we use a smaller patch length, stride, and look-back window: $PL_g = 16$, $STR_g = 8$, $PL_l = 4$, $STR_l = 2$, $L = 2S = 192$. The forecast horizon is set to $\{96, 192, 336, 720\}$ for each dataset. We use mean squared error and mean absolute error as metrics to compare performances of different architectures.

We now present the numerical result of our comprehensive experiments, as well as an ablation study to showcase the importance of each module, and a computation efficiency study comparing canonical architectures, SST, and S2TX.

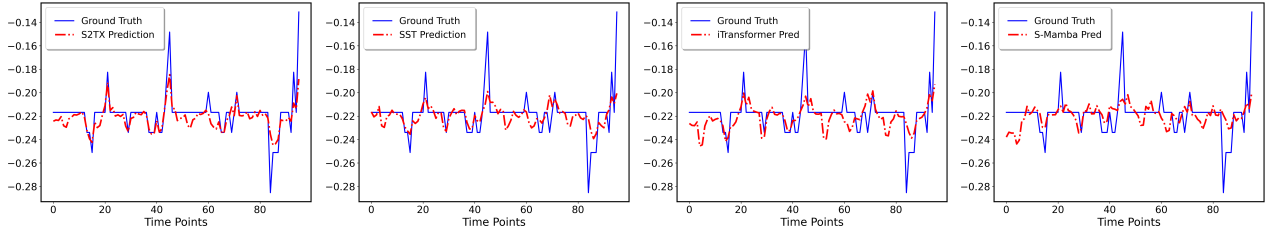


Figure 5. Empirical time series versus predicted time series across different architecture. S2TX can better capture the variation of the variable over time.

5.1. Benchmark Results

The performance of 9 different architectures on 7 benchmark datasets and 4 different prediction horizons is presented in Table 1. **Our method S2TX achieves SOTA performance across all benchmark datasets.** In particular, compared to the previous SOTA model SST, S2TX demonstrates consistent improvements on most datasets and performs on par on the weather dataset. For instance, S2TX achieves an 8.4% improvement on the ETTh1 dataset with a prediction horizon of 720. Moreover, even on the weather dataset, S2TX significantly surpasses other baseline models. The SOTA performance, together with our ablation studies in section 5.2, suggests that the two novel aspect of S2TX, the cross-variate global features, and the cross-attentional local features, are indeed important for accurately forecasting multivariate time series.

Guided by cross-variate global context, S2TX demonstrates a superior ability to capture local variations. Figure 5 presents a random segment of test time prediction from the electricity dataset on a randomly selected variate, comparing the performance of S2TX, SST, iTransformer, and S-Mamba. S2TX precisely approximates abrupt spikes while the accurate predictions of local variation are less apparent in predictions of other models.

5.2. Ablation and Robustness Studies

Ablation on Model Components. We perform ablation studies by removing key components of S2TX. To first assess the impact of cross-variate communication in learning global context, we input the patch sequence of each variate separately into the global model, rather than using the concatenated cross-variate patch sequence. Second, to evaluate the effectiveness of the context-local cross-attention mechanism, we remove cross-attention and instead concatenate the global context and local features before the final linear head. Finally, we remove both mechanisms to evaluate their combined effect. We conduct ablation studies on the ETTh1 and ETTm1 datasets and report the MSE metric, averaged across four different prediction lengths. As shown in Figure 6, the global-local cross-attention contributes the

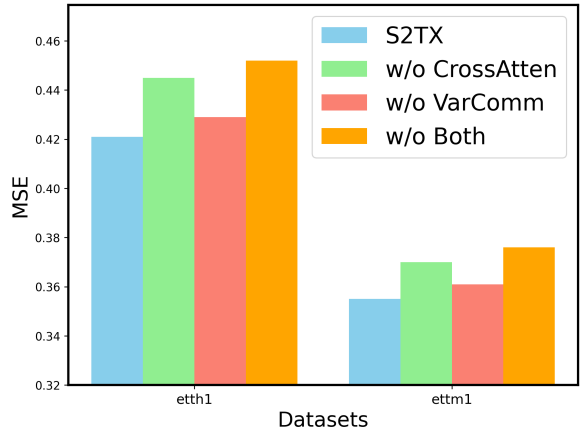


Figure 6. Ablation study on different components of S2TX tested on ETTh1 and ETTm1 datasets. The efficacy of each component of the proposed architectures is measured by the degradation of performance after each (or both) component(s) was excluded.

most to the overall improvement of S2TX, while variable communication also positively influences the results.

Robustness to Missing Values. In real-world multivariate time series datasets, it is common to observe missing values. Unlike traditional tabular data where a few elements are missing, missing values in time series could exist for small periods of sequences. In this set of robustness experiments, we randomly select small sequences of 4 time steps to be missing and interpolate these randomly missing periods with the value of the last observed time step. In Table 2, we present the MSE of different architectures under various percentage of missing values. We show that S2TX, with the addition of cross-variate global context and the cross-attentional global-local feature interplay, is highly robust compared to SST, which showed much-worsened degradation as the percentage of missing value increases.

5.3. Memory and Runtime Analysis

To ensure a fair runtime comparison, we evaluate S2TX alongside SST, the vanilla Transformer, and Mamba on a

Miss Ratio	S2TX	SST
0%	0.421(-0.0%)	0.439(-0.0%)
4%	0.424(-0.7%)	0.440(-0.2%)
8%	0.425(-0.9%)	0.443(-0.9%)
16%	0.424(-0.7%)	0.450(-2.5%)
24%	0.429(-1.9%)	0.468(-6.6%)
32%	0.431(-2.3%)	0.471(-7.0%)
40%	0.441(-4.7%)	0.499(-13.4%)

Table 2. Performance on ETTh1 with increasing proportion of missing values; results are MSE averaged over all four prediction horizons.

single NVIDIA RTX 6000 Ada Generation GPU. The two versions of S2TX and SST correspond to configurations with either a fixed patch number or a fixed stride length. In the former case, the patch number remains constant regardless of sequence length, whereas in the latter case, the patch number increases proportionally with sequence length.

It is important to note that we compare against the vanilla Transformer and Mamba, rather than their inverted versions, as the respective attention and selective mechanisms in the inverted versions operate on the variate dimension. As the look-back window sequence length increases, the memory usage and runtime of the Transformer grow exponentially, reaching the GPU’s memory limit when the sequence length hits 2000. In contrast, Mamba scales linearly in both memory and time metrics.

Both S2TX and SST scale more efficiently than Mamba, owing to the fixed short local look-back window combined with the patching technique, which effectively reduces the sequence length by a factor of the stride length. The complexity experiment result is presented in Figure 7. Consistent to the runtime analysis in section 5.3, when the global patch number is fixed, both S2TX and SST achieve nearly constant runtime complexity. However, when comparing S2TX to SST, SST scales slightly better due to the additional cross-attention mechanism in S2TX.

6. Discussion and Future Work

In this work, we introduce a new architecture, *State-Space Transformer with cross-attention* (S2TX), for multivariate time series modeling. We first noted that the multi-scale patching methods, although enhance the learning of temporal dependencies, neglect the cross-variate correlation—a crucial aspect of multivariate time series modeling. Also, global and local patches are processed independently, overlooking the global and local interactions that occur in many real-world scenarios. We propose a novel cross-attention based architecture that integrates state space models and transformers. This cross-attention architecture, combined with patchification, fully leverages the strengths of Mamba

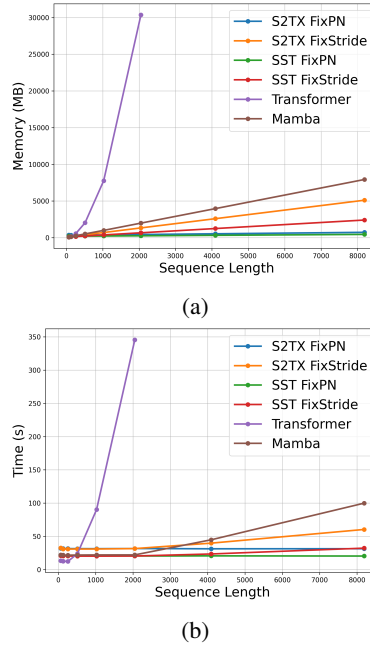


Figure 7. Memory and run-time comparison between S2TX and other canonical architectures.

and transformers by integrating cross-variate global features from Mamba with the local features of the transformer. Our architecture generally improves over current state-of-the-art in various datasets and 4 different prediction horizons. The SOTA performance of S2TX is not only achieved with a low memory footprint and fast computation runtime but also demonstrated robust performance when facing time series with sequences of missing values. Given these advantages, S2TX unlocks new possibilities for time series forecasting by effectively capturing cross-variate correlations and global-local feature interactions.

Limitations. Several limitations exist in our current architectures. One key limitation is that cross-variate correlations are not explicitly explored at a local level. Although S2TX maintains low memory usage and fast runtime, incorporating local cross-variate correlations could further enhance performance. Another limitation is the lack of diversity in the multi-scale approach. The current architecture only deals with global and local patches with no learning of the intermediate scales. Intermediate time scales, however, could be important for extremely long sequences where the difference in time scales between global and local contexts is dramatic. Incorporating multiple time scales within an architecture while remaining lightweight is still unsolved. We leave these for future works.

Impact Statement This paper presents work whose goal is to advance the field of Machine Learning. There are many potential societal consequences of our work, none of which

we feel must be specifically highlighted here.

References

- Ahamed, M. A. and Cheng, Q. Timemachine: A time series is worth 4 mambas for long-term forecasting. *arXiv preprint arXiv:2403.09898*, 2024.
- Angryk, R. A., Martens, P. C., Aydin, B., Kempton, D., Mahajan, S. S., Basodi, S., Ahmadzadeh, A., Cai, X., Filali Boubrahimi, S., Hamdi, S. M., et al. Multivariate time series dataset for space weather data analytics. *Scientific data*, 7(1):227, 2020.
- Bahdanau, D. Neural machine translation by jointly learning to align and translate. *arXiv preprint arXiv:1409.0473*, 2014.
- Bloomfield, P. *Fourier analysis of time series: an introduction*. John Wiley & Sons, 2004.
- Box, G. E., Jenkins, G. M., Reinsel, G. C., and Ljung, G. M. *Time series analysis: forecasting and control*. John Wiley & Sons, 2015.
- Chen, C.-F. R., Fan, Q., and Panda, R. Crossvit: Cross-attention multi-scale vision transformer for image classification. In *Proceedings of the IEEE/CVF international conference on computer vision*, pp. 357–366, 2021.
- Durbin, J. and Koopman, S. J. *Time series analysis by state space methods*, volume 38. OUP Oxford, 2012.
- Gers, F. A., Schmidhuber, J., and Cummins, F. Learning to forget: Continual prediction with lstm. *Neural computation*, 12(10):2451–2471, 2000.
- Gong, Z., Tang, Y., and Liang, J. Patchmixer: A patch-mixing architecture for long-term time series forecasting. *arXiv preprint arXiv:2310.00655*, 2023.
- Graves, A., Mohamed, A.-r., and Hinton, G. Speech recognition with deep recurrent neural networks. In *2013 IEEE international conference on acoustics, speech and signal processing*, pp. 6645–6649. Ieee, 2013.
- Gu, A. and Dao, T. Mamba: Linear-time sequence modeling with selective state spaces. *arXiv preprint arXiv:2312.00752*, 2023.
- Gu, A., Dao, T., Ermon, S., Rudra, A., and Ré, C. Hippo: Recurrent memory with optimal polynomial projections. *Advances in neural information processing systems*, 33: 1474–1487, 2020.
- Gu, A., Goel, K., and Ré, C. Efficiently modeling long sequences with structured state spaces. *arXiv preprint arXiv:2111.00396*, 2021.
- Horn, R. A. and Johnson, C. R. *Matrix analysis*. Cambridge university press, 2012.
- Hsieh, W. W. Nonlinear multivariate and time series analysis by neural network methods. *Reviews of Geophysics*, 42(1), 2004.
- Hyndman, R. *Forecasting: principles and practice*. OTexts, 2018.
- Koop, G., Korobilis, D., et al. Bayesian multivariate time series methods for empirical macroeconomics. *Foundations and Trends® in Econometrics*, 3(4):267–358, 2010.
- Lai, G., Chang, W.-C., Yang, Y., and Liu, H. Modeling long-and short-term temporal patterns with deep neural networks. In *The 41st international ACM SIGIR conference on research & development in information retrieval*, pp. 95–104, 2018.
- Li, Z., Qi, S., Li, Y., and Xu, Z. Revisiting long-term time series forecasting: An investigation on linear mapping. *arXiv preprint arXiv:2305.10721*, 2023.
- Lieber, O., Lenz, B., Bata, H., Cohen, G., Osin, J., Dalmedigos, I., Safahi, E., Meïrom, S., Belinkov, Y., Shalev-Shwartz, S., et al. Jamba: A hybrid transformer-mamba language model. *arXiv preprint arXiv:2403.19887*, 2024.
- Liu, Y., Hu, T., Zhang, H., Wu, H., Wang, S., Ma, L., and Long, M. itransformer: Inverted transformers are effective for time series forecasting. *arXiv preprint arXiv:2310.06625*, 2023.
- Nerlove, M. Time series analysis, forecasting, and control., 1971.
- Nguyen, H. M., Turk, P. J., and McWilliams, A. D. Forecasting covid-19 hospital census: A multivariate time-series model based on local infection incidence. *JMIR Public Health and Surveillance*, 7(8):e28195, 2021.
- Nie, Y., Nguyen, N. H., Sinthong, P., and Kalagnanam, J. A time series is worth 64 words: Long-term forecasting with transformers. *arXiv preprint arXiv:2211.14730*, 2022.
- Vaswani, A. Attention is all you need. *Advances in Neural Information Processing Systems*, 2017.
- Wang, Z., Kong, F., Feng, S., Wang, M., Yang, X., Zhao, H., Wang, D., and Zhang, Y. Is mamba effective for time series forecasting? *Neurocomputing*, 619:129178, 2025.
- Wu, H., Xu, J., Wang, J., and Long, M. Autoformer: Decomposition transformers with auto-correlation for long-term series forecasting. *Advances in neural information processing systems*, 34:22419–22430, 2021.

- Wu, H., Hu, T., Liu, Y., Zhou, H., Wang, J., and Long, M. Timesnet: Temporal 2d-variation modeling for general time series analysis. *arXiv preprint arXiv:2210.02186*, 2022.
- Xu, X., Chen, C., Liang, Y., Huang, B., Bai, G., Zhao, L., and Shu, K. Sst: Multi-scale hybrid mamba-transformer experts for long-short range time series forecasting, 2024.
- Yang, H., Hasan, A., Ng, Y., and Tarokh, V. Neural mckean-vlasov processes: Distributional dependence in diffusion processes. In *International Conference on Artificial Intelligence and Statistics*, pp. 262–270. PMLR, 2024.
- Zeng, A., Chen, M., Zhang, L., and Xu, Q. Are transformers effective for time series forecasting? In *Proceedings of the AAAI conference on artificial intelligence*, volume 37-9, pp. 11121–11128, 2023.
- Zhang, Y. and Yan, J. Crossformer: Transformer utilizing cross-dimension dependency for multivariate time series forecasting. In *The eleventh international conference on learning representations*, 2023.
- Zhou, H., Zhang, S., Peng, J., Zhang, S., Li, J., Xiong, H., and Zhang, W. Informer: Beyond efficient transformer for long sequence time-series forecasting. In *Proceedings of the AAAI conference on artificial intelligence*, volume 35, pp. 11106–11115, 2021.
- Zhou, T., Ma, Z., Wen, Q., Wang, X., Sun, L., and Jin, R. Fedformer: Frequency enhanced decomposed transformer for long-term series forecasting. In *International conference on machine learning*, pp. 27268–27286. PMLR, 2022.

A. Algorithm

Algorithm 1 S2TX: State-Space Transformer With Cross Attention

Input: Loss function \mathcal{L} , global model g_ϕ , local model f_ψ , number of total training epochs T , dataset D , learning rate η , global patch length, stride, and window PL_g, Str_g, L , local patch length, stride, and window PL_l, Str_l, S .

Output: ϕ, ψ .

```

1: Initialize parameters  $\phi, \psi$ .
2: for  $i \leftarrow 0$  to  $T - 1$  do
3:   Shuffle dataset  $D$ .
4:   for each minibatch  $(X, Y) \subset D$  do
5:      $\tilde{X}_g, \tilde{X}_l \leftarrow \text{Patchify}(X; PL_g, Str_g, L), \text{Patchify}(X; PL_l, Str_l, S)$ 
6:      $Y_g \leftarrow g_\phi(\tilde{X}_g)$ 
7:      $\hat{Y} \leftarrow f_\psi(Y_g, \tilde{X}_l)$ 
8:      $\phi \leftarrow \phi - \eta \nabla_\phi \mathcal{L}(\hat{Y}, Y)$ 
9:      $\psi \leftarrow \psi - \eta \nabla_\psi \mathcal{L}(\hat{Y}, Y)$ 
10:   end for
11: end for
12: return  $\phi, \psi$ 

```

B. Dataset Description

In this section, we describe the dataset used in our experiments in Table 1. Our experiments include 7 widely used real world multivariate time series. Table 3 presents the number of variables and number of timesteps.

- The ETT dataset (Zhou et al., 2021) records 7 factors that related to electric transformers from July 2016 to July 2018. The ETT dataset includes 4 subsets where ETTh1 and ETTh2 are recorded hourly and ETTm1 and ETTm2 are recorded every 15 minutes.
- The exchange dataset (Lai et al., 2018) tracks the daily exchange rates of eight foreign countries including Australia, British, Canada, Switzerland, China, Japan, New Zealand, and Singapore ranging from 1990 to 2016.
- The weather dataset (Wu et al., 2021) includes 21 different meteorological features measured every 10 minutes by the Weather Station at the Max Planck Institute for Biogeochemistry.
- The ECL dataset (Lai et al., 2018) records electricity consumption in kWh every 15 minutes from 2012 to 2014, for 321 clients. The data is converted to reflect hourly consumption.

	ETTh1	ETTh2	ETTm1	ETTm2	Exchange	Weather	ECL
# Variables	7	7	7	7	8	21	321
# Time steps	17420	17420	69680	69680	7588	52696	26304

Table 3. Table of Dataset summary including number of variables and number of time steps of each dataset.

C. Comparison with more benchmark architectures

In this section we present the full table of comparison that including two more baselines: Dlinear and FEDformer. Table 4 is organized similarly as Table 1.

S2TX: cross-attention Multi-Scale State-Space Transformer for Time Series Forecasting

	S2TX		SST		S-Mamba		TimeM		iTrans		RLinear		PatchTST		CrossF		TimesNet		DLinear		FEDformer	
	MSE	MAE	MSE	MAE	MSE	MAE	MSE	MAE	MSE	MAE	MSE	MAE	MSE	MAE	MSE	MAE	MSE	MAE	MSE	MAE	MSE	MAE
ETTh1																						
96	0.376	0.401	<u>0.381</u>	0.405	0.392	0.390	0.389	0.402	0.386	0.405	0.386	<u>0.395</u>	0.414	0.419	0.423	0.448	0.384	0.402	0.386	0.400	0.376	0.419
192	0.414	0.421	<u>0.430</u>	0.434	0.449	0.439	0.435	0.440	0.441	0.436	0.437	<u>0.424</u>	0.460	0.445	0.450	0.471	0.474	0.429	0.437	0.432	<u>0.420</u>	0.448
336	0.432	0.435	<u>0.443</u>	<u>0.446</u>	0.467	0.481	0.450	0.448	0.487	0.458	0.479	0.446	0.501	<u>0.466</u>	0.570	0.546	0.491	0.469	0.481	0.459	0.459	0.465
720	0.463	<u>0.473</u>	0.502	0.501	<u>0.475</u>	0.468	0.480	0.465	0.503	0.491	0.481	0.470	0.500	0.488	0.653	0.621	0.521	0.500	0.519	0.516	0.506	0.507
ETTh2																						
96	0.279	<u>0.340</u>	0.291	0.346	0.292	0.357	0.296	0.349	0.297	0.349	<u>0.288</u>	0.338	0.302	0.348	0.745	0.584	0.340	0.374	0.333	0.387	0.358	0.397
192	0.362	<u>0.395</u>	<u>0.369</u>	<u>0.397</u>	0.380	0.402	0.371	0.400	0.380	0.400	0.374	0.390	0.388	0.400	0.877	0.656	0.402	0.414	0.477	0.476	0.429	0.439
336	0.337	0.385	<u>0.374</u>	<u>0.414</u>	0.391	0.420	0.402	0.449	0.428	0.432	0.415	0.426	0.426	0.433	1.043	0.731	0.452	0.452	0.594	0.541	0.496	0.487
720	0.395	0.430	<u>0.419</u>	0.447	0.437	0.455	0.425	<u>0.438</u>	0.427	0.445	0.420	0.440	0.431	0.446	1.104	0.763	0.462	0.468	0.831	0.657	0.463	0.474
ETTm1																						
96	0.289	0.343	<u>0.298</u>	<u>0.355</u>	0.311	0.380	0.312	0.371	0.334	0.368	0.355	0.376	0.329	0.367	0.404	0.426	0.338	0.375	0.345	0.372	0.379	0.419
192	0.338	0.371	<u>0.347</u>	<u>0.381</u>	0.389	0.419	0.365	0.409	0.377	0.391	0.391	0.392	0.367	0.385	0.450	0.451	0.374	0.387	0.380	0.389	0.426	0.441
336	0.370	0.390	<u>0.374</u>	<u>0.397</u>	0.401	0.417	0.421	0.410	0.426	0.420	0.424	0.415	0.399	0.410	0.532	0.515	0.410	0.411	0.413	0.413	0.445	0.459
720	0.423	0.418	<u>0.429</u>	<u>0.428</u>	0.488	0.476	0.496	0.437	0.491	0.459	0.487	0.450	0.454	0.439	0.666	0.589	0.478	0.450	0.474	0.453	0.543	0.490
ETTm2																						
96	0.168	<u>0.260</u>	0.176	0.264	0.191	0.301	0.185	0.290	0.180	0.264	0.182	0.265	<u>0.175</u>	0.259	0.287	0.366	0.187	0.267	0.193	0.292	0.203	0.287
192	<u>0.235</u>	0.298	0.231	0.303	0.253	0.312	0.292	0.309	0.250	0.309	0.246	0.304	0.241	<u>0.302</u>	0.414	0.492	0.249	0.309	0.284	0.362	0.269	0.328
336	0.274	0.327	<u>0.290</u>	<u>0.339</u>	0.298	0.342	0.321	0.367	0.311	0.348	0.307	0.342	0.305	0.343	0.597	0.542	0.321	0.351	0.369	0.427	0.325	0.366
720	0.376	0.393	<u>0.388</u>	<u>0.398</u>	0.409	0.407	0.401	0.400	0.412	0.407	0.407	0.398	0.402	0.400	1.730	1.042	0.408	0.403	0.554	0.522	0.421	0.415
Exchange																						
96	0.085	<u>0.205</u>	0.097	0.222	<u>0.086</u>	0.206	0.089	0.208	0.091	0.211	0.088	0.209	0.087	0.202	0.095	0.218	0.093	0.211	0.101	0.223	0.105	0.226
192	0.179	0.303	0.191	0.315	0.182	0.304	0.184	0.309	0.182	0.303	0.188	0.311	<u>0.180</u>	0.305	0.193	0.318	0.194	0.315	0.203	0.324	0.211	0.338
336	0.311	0.402	0.337	0.424	0.330	0.416	0.333	0.416	0.337	0.421	0.346	0.423	<u>0.318</u>	<u>0.407</u>	0.359	0.429	0.358	0.433	0.369	0.445	0.370	0.441
720	0.858	0.696	0.877	0.706	0.865	0.702	0.870	<u>0.701</u>	<u>0.862</u>	0.703	0.913	0.717	0.863	0.703	0.918	0.721	0.880	0.719	0.909	0.711	0.912	0.718
Weather																						
96	0.150	0.199	<u>0.153</u>	<u>0.205</u>	0.169	0.221	0.174	0.218	0.174	0.214	0.192	0.232	0.177	0.218	0.158	0.230	0.172	0.220	0.196	0.255	0.217	0.296
192	0.194	0.242	<u>0.196</u>	<u>0.244</u>	0.205	0.248	0.200	0.258	0.221	0.254	0.240	0.271	0.225	0.259	0.206	0.277	0.219	0.261	0.237	0.296	0.276	0.336
336	<u>0.252</u>	<u>0.288</u>	0.246	0.283	0.288	0.299	0.280	0.299	0.278	0.296	0.292	0.307	0.278	0.297	0.272	0.335	0.280	0.306	0.283	0.335	0.339	0.380
720	0.313	0.333	<u>0.314</u>	<u>0.334</u>	0.335	0.369	0.352	0.359	0.358	0.347	0.364	0.353	0.354	0.348	0.398	0.418	0.365	0.359	0.345	0.381	0.403	0.428
ECL																						
96	0.134	0.231	<u>0.141</u>	<u>0.239</u>	0.157	0.255	0.156	0.240	0.148	0.240	0.201	0.281	0.181	0.270	0.219	0.314	0.168	0.272	0.197	0.282	0.193	0.308
192	0.153	0.248	<u>0.159</u>	<u>0.255</u>	0.188	0.271	0.161	0.268	0.162	0.253	0.201	0.283	0.188	0.274	0.231	0.322	0.184	0.289	0.196	0.285	0.201	0.315
336	0.170	0.266	<u>0.171</u>	<u>0.268</u>	0.192	0.275	0.195	0.272	0.178	0.269	0.215	0.298	0.204	0.293	0.246	0.337	0.198	0.300	0.209	0.301	0.214	0.329
720	0.201	0.293	<u>0.208</u>	<u>0.300</u>	0.241	0.339	0.231	0.307	0.225	0.317	0.257	0.331	0.246	0.324	0.280	0.363	0.220	0.320	0.245	0.333	0.246	0.355

Table 4. Comprehensive comparison across various dataset with additional baselines. The **bolded** results denote the best performance, and the underlined results indicate the second best.